Applied Surface Science 256 (2010) 7472–7477

Contents lists available at ScienceDirect

Applied Surface Science

journal homepage: www.elsevier.com/locate/apsusc

Synthesis of ZnO compound nanostructures via a chemical route for photovoltaic applications

Y.F. Zhu[a,b], W.Z. Shen[a,*]

[a] Laboratory of Condensed Matter Spectroscopy and Opto-Electronic Physics, Institute of Solar Energy, Department of Physics, Shanghai Jiao Tong University, 1954 Hua Shan Road, Shanghai 200030, People's Republic of China
[b] Faculty of Mechanical Engineering, Huaiyin Institute of Technology, 1 Mei Cheng Road, Jiangsu 223003, People's Republic of China

ARTICLE INFO

Article history:
Received 23 September 2009
Received in revised form 27 May 2010
Accepted 27 May 2010
Available online 4 June 2010

PACS:
81.07.Bc
73.50.Pz
81.16.Be

Keywords:
Nanostructures
Semiconductors
Chemical synthesis
Photoconductivity and photovoltaics

ABSTRACT

A facile, low-temperature, and low-cost chemical route has been developed to prepare ZnO nanowire and nanosphere compound structures. The morphology, structure, and composition of the yielded products have been examined by field-emission scanning electron microscopy, transmission electron microscopy, and X-ray diffraction measurements. We have systematically investigated the optical properties of the ZnO nanostructures by micro-Raman, photoluminescence, and transmission spectroscopy. The results demonstrate that the yielded ZnO nanostructures possess good optical quality with high light absorption. We have further successfully employed the obtained ZnO compound nanostructures in dye-sensitized solar cells. The light-to-electricity conversion results show that the compound nanostructure exhibits a significant enhancement of short-circuit current density due to the increased surface area and light scattering in the compound nanostructures. The present chemical route provides a simple way to synthesize various compound nanostructures with high surface area for nanodevice applications.

1. Introduction

The synthesis and application of nanostructures in dye-sensitized solar cells (DSSCs) have attracted much attention, since DSSCs were firstly reported by O'Regan and Grätzel [1]. Up to now, various metal oxide nanostructures such as TiO_2, ZnO, Fe_2O_3, ZrO_2, Nb_2O_5, Al_2O_3, and CeO_2 have been successfully employed as photoelectrodes in DSSCs [2–14]. Among the above-mentioned metal oxide nanostructures, the study of TiO_2 and ZnO is of particular interest due to the fact that they are the best candidates as photoelectrode used in DSSCs. At present, TiO_2 nanoparticle-based DSSCs demonstrate the highest efficiency (~11%) [3]. Compared with TiO_2, ZnO shows higher electron mobility with similar bandgap and conduction band energies. Therefore, ZnO is an alternative candidate for high efficient DSSCs.

There are a variety of reports on the application of ZnO nanostructures as photoelectrodes in DSSCs [11–20]. Among the various nanostructures, the application of highly ordered ZnO nanowires in DSSCs is of great interest. The single crystalline ZnO nanowires have been proved to significantly improve the electron transport in the photoelectrode films by providing a direct conduction pathway for the photogenerated electrons [15], as schematically demonstrated in Fig. 1(a). However, the ZnO nanowires-based DSSCs usually show low current density compared with that made of random nanoparticle network. The low current density in the ZnO nanowire photoelectrode is due to the fact that the surface area of the ZnO nanowire photoelectrode is limited [21,22]. On the other hand, as for the ZnO nanospheres-based DSSCs [Fig. 1(b)], although the film made of ZnO nanospheres can provide large surface area, the photogenerated electrons will interact with a lot of traps when they walk through the random network [15]. It is therefore interesting to synthesize photoelectrodes made of nanowire and nanosphere compound structures, in which one keeps two merits of the previous mentioned structures, as shown in Fig. 1(c). In this kind of photoelectrode, the surface area can be increased without significantly slowing down the electron transport in photoelectrode films. The overall efficiency of the compound nanostructures-based DSSCs is expected to be increased.

In this paper, we have developed a simple and low-cost chemical route to prepare ZnO nanowire and nanosphere compound nanostructures. The key point of the present method is that we employ a certain concentration of trisodium citrate to control the nucleation and growth rate of ZnO crystal for producing nanospheres in the interstices between the nanowires. There are two purposes for the

* Corresponding author. Fax: +86 21 54747552.
E-mail address: wzshen@sjtu.edu.cn (W.Z. Shen).

0169-4332/$ – see front matter © 2010 Elsevier B.V. All rights reserved.
doi:10.1016/j.apsusc.2010.05.092

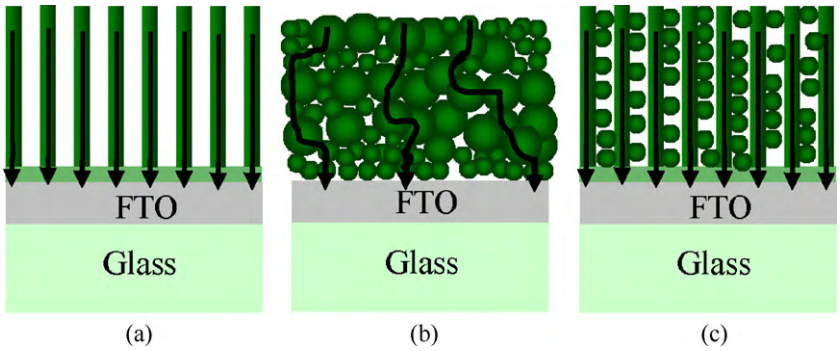

Fig. 1. Schematic diagram of photoelectrodes made of (a) nanowires, (b) nanoparticles, and (c) nanowire and nanosphere compound nanostructures.

deposition of nanospheres in the interstices between the nanowire arrays. On one hand, the surface area of the photoelectrode will be increased after filling the interstices between the nanowires. On the other hand, the introduction of nanospheres in the photoelectrode will promote the light scattering and enhance the photon absorption. Compared with the nanowires-based counterpart, the compound nanostructure DSSC exhibits a significant enhancement of the short-circuit current density. We will show that the improved performance does benefit from the enhanced light absorption by depositing nanospheres in the interstices between the nanowires.

2. Experimental details

2.1. Synthesis of ZnO nanowire arrays on conductive substrates

A simple and low-cost chemical route has been adopted to prepare ZnO nanowire arrays. FTO (fluorine doped tin oxide, SnO_2:F) glass cleaned by sonication in ethanol and water was employed as substrate. The seed layer on the FTO glass was formed by thermally decomposing zinc acetate at 350 °C. In a typical process, FTO glass is wet with a droplet of 0.005 M zinc acetate dihydrate in ethanol, and then dry in a conventional laboratory oven. The dry substrate with a thin layer of zinc acetate is heated to 350 °C in a Muffle furnace in an air atmosphere. In order to make sure that the FTO glass is covered by a layer of ZnO nanocrystal, we repeat the above step two times. Next, the seeded FTO glass substrate was employed to grow highly ordered ZnO nanowires by immersing the substrate in an aqueous solution containing 10 mM zinc nitrate hexahydrate ($Zn(NO_3)_2{\cdot}6H_2O$) and 10 mM hexamethylenetetramine ($C_6H_{12}N_4$). During the growth process, the temperature of the solution was maintained at 92 °C.

2.2. Synthesis of ZnO nanowire and nanosphere compound structures

In this step, a facile, low-temperature, and low-cost synthetic method has been developed to prepare nanospheres. Because the citrate ions can strongly bind to the Zn atoms on the ZnO (0 0 1) surface and limit the growth rate of ⟨0 0 1⟩ orientation [23], high concentration of trisodium citrate is used in this step to control the nucleation and growth rate of ZnO crystal. The strategy employed here to produce spherical structure is similar to that reported in the previous work [24]. To synthesize compound structures, we transferred FTO substrate with the first step prepared highly ordered ZnO nanowires into a glass bottle containing of 25 mM $Zn(NO_3)_2{\cdot}6H_2O$, 1.7 mM $C_6H_5Na_3O_7{\cdot}2H_2O$, and 0.25 mL ammonia with concentration of 25%. During this step, the solution was heated to 85 °C for 4.5 h. The final products on the substrates were washed repeatedly and then dried at 60 °C for the next step to prepare DSSCs and further characterization.

2.3. Characterization of the samples

The morphology and structure of the samples were characterized using a field-emission scanning electron microscope (FESEM; Philips XL30FEG) with an accelerating voltage of 5 kV and a high-resolution transmission electron microscope (HRTEM; JEOL JEM-2100F). The selected area electron diffraction (SAED) and energy-dispersive X-ray (EDX) microanalysis were also performed during the transmission electron microscope (TEM) measurements. X-ray diffraction (XRD) was carried out on a D-max/2550 (Rigaku) X-ray diffractometer system equipped with a Cu Kα source (λ = 1.5406 Å). Micor-Raman and photoluminescence (PL) spectra were recorded at room temperature by a Jobin Yvon LabRAM HR 800UV micro-Raman/PL system under an Ar^+ (514.5 nm) and He–Cd (325.0 nm) laser excitation, respectively. In order to demonstrate that deposition of ZnO nanospheres in the interstices between the nanowires can improve light harvesting, we perform the optical transmission measurements on a Jobin Yvon 460 monochromator in the wavelength range of 400–900 nm.

2.4. Fabrication and characterization of DSSCs

The prepared ZnO photoelectrodes were sensitized by immersing them in 0.5 mM N719 dye in anhydrous ethanol solution for 1.5 h. The counter electrode was a FTO glass coated with a layer of sputtered Pt. In order to prevent short circuit of the two electrodes, we have separated the photoanode and the counter electrode by a spacer (100 μm in thickness) and pressed by clamps. The electrolyte was introduced into the two electrodes by capillary action. The electrolyte solution used here was consisting of 0.6 M tetra-butylammonium iodide, 0.1 M lithium iodide, 0.1 M iodine, and 0.5 M 4-tert-butylpyridine in acetonitrile. The photocurrent–photovoltage measurements were performed using a CHI-660 electrochemical working station by varying an external load voltage. A Newport-Oriel 69911 (150 W) solar light simulator was used as a white light source. The intensity of incident light was calibrated to be 100 mW/cm^2 by radiometer. During measurements, a mask was adopted to create an exposed area of 0.15 cm^2 for all samples (the device size is about 1 cm × 2 cm).

3. Results and discussion

3.1. Structural characterization of highly ordered ZnO nanowires

Fig. 2(a) shows cross-sectional SEM image of the ZnO nanowire array. It is clear that the alignment is good and the length of nanowires is about 7.5 μm. The highly ordered ZnO nanowires were directly grown on the FTO glass substrates. Fig. 2(b) demonstrates the top-view SEM image of the ZnO nanowire array. From the figure, one can see that there are large interstices between the nanowires.

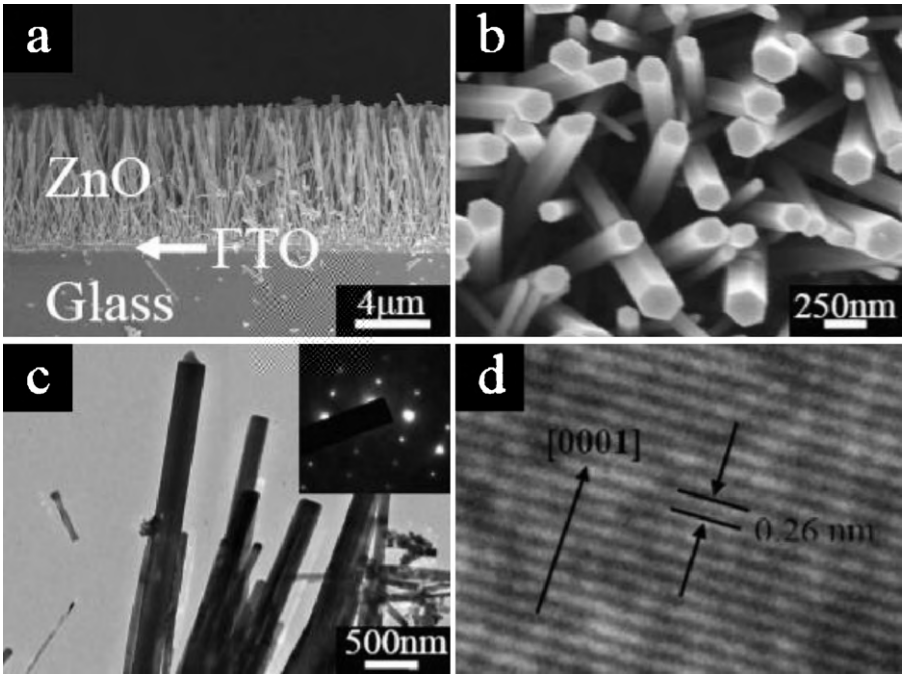

Fig. 2. (a) Cross-sectional and (b) top-view SEM images of the ZnO nanowire array; (c) TEM image of the ZnO nanowires (inset: the corresponding selected area electron diffraction pattern); and (d) HRTEM image of the ZnO nanowire.

As a result, the surface area of this kind of photoelectrode is limited. If the interstices between ZnO nanowires could be filled with other ZnO nanostructures, the surface area of the photoelectrode would be increased. It is reported that the diameter and the density of the nanowires grown on the FTO substrate have significant impact on the performance of DSSCs [25]. From Fig. 2(b), one can easily obtain the diameter and density of the yielded nanowires is about 150 nm and 10^{13} m^{-2}, respectively.

TEM measurements have also been carried out for further investigation of the ZnO nanowires. Fig. 2(c) shows the TEM image of the obtained ZnO nanowire array, which is consistent with the SEM observation shown in Fig. 2(a). The corresponding SAED pattern displayed in the inset of Fig. 2(c) suggests the single crystallinity nature of the yielded ZnO nanowires. The HRTEM image shown in Fig. 2(d) confirms that the obtained ZnO nanowires are single crystalline. The lattice fringe spacing in Fig. 2(d) is measured to be 0.26 nm, which corresponds to the distance between two adjacent ZnO (0 0 0 2) planes, indicating that [0 0 0 1] is the growth direction of the nanowires [26].

3.2. Structural characterization of ZnO nanowire and nanosphere compound structures

The main achievement in the present work is to synthesize nanowire and nanosphere compound structures for increasing the short-circuit current density of the ZnO DSSCs. As we know, the direct fabrication of ZnO nanowire and nanosphere compound structures remains a significant challenge. The difficulty lies in the fact that ZnO nanospheres do not easy to obtain and fill the interstices between the nanowires without sticking to the top-most nanowires. Since solution can easily infiltrate the interstices between the nanowires, the synthesis of nanowire and nanosphere compound structures can be realized by using the solution that produces ZnO nanospheres, where the total ZnO surface area of the photoelectrode increases.

We have successfully synthesized the ZnO nanowire and nanosphere compound structures. Fig. 3(a) presents the low-magnification FESEM image of the ZnO compound nanostructures. It is clear that large-scale uniform nanospheres have been obtained. The diameter of the nanospheres is about 400 nm. From the high-magnification FESEM image of the compound nanostructures [Fig. 3(b)], one can see that the nanospheres do deposit in the interstitial space between the ZnO nanowires. Though the Brunauer–Emmett–Teller (BET) surface area measurement and/or dye loading characterization can demonstrate the total surface area of ZnO nanocomposites, the increase of ZnO surface area is obvious after forming ZnO compound nanostructures. Before depositing ZnO nanospheres in the interstices between the ZnO nanowires, the total surface area of the ZnO nanowires-based photoelectrode [Fig. 2(b)] is the sum of the surface area of ZnO nanowires grown on FTO substrate. After depositing nanospheres in the interstices between the ZnO nanowires, the total surface area of the ZnO compound nanostructures-based photoelectrode [Fig. 3(b)] is the sum of the surface area of ZnO nanowires and the surface area of ZnO nanospheres. Therefore, the surface area of the photoelectrode is increased by filling the interstitial space. Fig. 3(c) and (d) shows the side-view SEM image of the obtained ZnO compound nanostructures at the edge of photoelectrode. We can also observe that ZnO nanospheres have been filled in the interstitial space and some flake-like structures are grown on the ZnO nanowires at the edge of the photoelectrodes. These flake-like structures deposited on the nanowires also increase the surface area of the photoelectrode, which will contribute to the increase of short-circuit current density of the yielded DSSCs.

XRD characterization can further demonstrate the crystal structure of the obtained compound nanostructures. Fig. 4 represents the diffraction patterns of a bare FTO glass [shown in Fig. 4(a)], highly ordered ZnO nanowires grown on a FTO glass [Fig. 4(b)], ZnO nanowire and nanosphere compound structures on a FTO glass [Fig. 4(c)], and ZnO nanospheres prepared on a bare FTO glass substrate [Fig. 4(d)]. From Fig. 4(a), it can be clearly observed that only the peaks corresponding to the tetragonal SnO_2 structure [powder diffraction file (PDF) No. 77-0450] are detected, confirming that the bare FTO are consist of polycrystalline SnO_2. Since we have employed bare FTO glass as substrate, the diffraction patterns corresponding to SnO_2 have also been detected in the

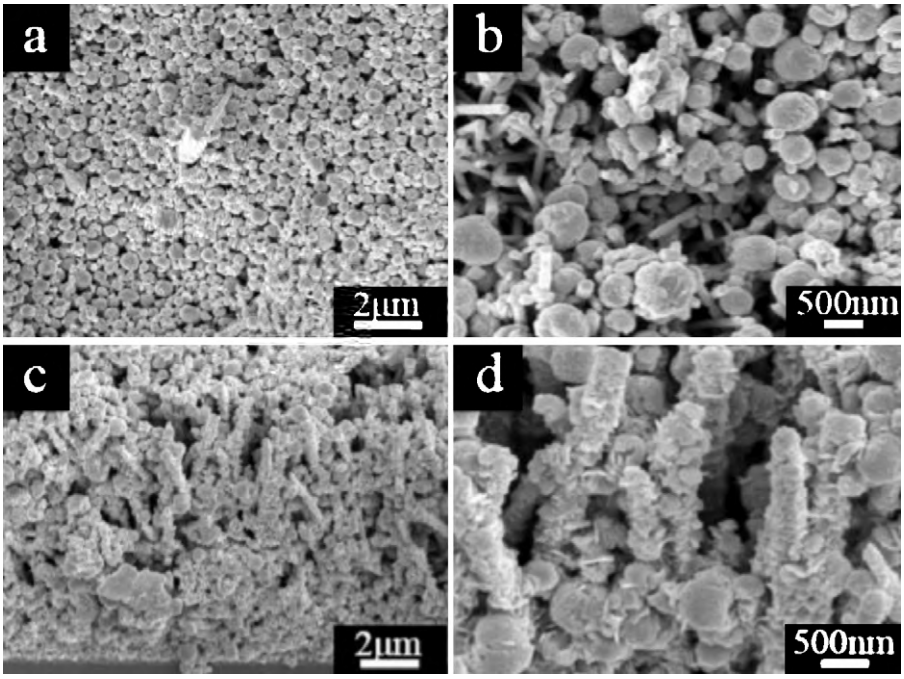

Fig. 3. (a) Low- and (b) high-magnification top-view FESEM images of the ZnO nanowire and nanosphere compound nanostructures; (c) low- and (d) high-magnification side-view SEM image of the ZnO compound nanostructures at the edge of photoelectrode.

following synthesized nanostructures. The diffraction peaks of the hexagonal ZnO structure [PDF No. 36-1451] appear after the ZnO nanowires grown on a bare FTO glass [Fig. 4(b)], indicating the formation of a layer of ZnO on the FTO substrate. The obtained ZnO nanowires show a dominant strong (0 0 0 2) peak, indicating the film exhibits a preferred orientation of (0 0 0 2) direction, which is consistent with the SEM results shown in Fig. 2(a). After depositing ZnO nanospheres in the interstices between the nanowires, the other diffraction peaks corresponding to the hexagonal ZnO became strong [Fig. 4(c)]. This is originated from the polycrystalline nature of the newly deposited ZnO nanospheres. In order to further confirm this argument, we have conducted the XRD characterization of ZnO nanospheres deposited on a bare FTO [Fig. 4(d)], where the obtained ZnO nanospheres are polycrystalline without any dominant orientation.

3.3. Optical properties of the yielded ZnO nanostructures

To examine the optical properties of these yielded ZnO nanostructures, we first perform the room-temperature micro-Raman

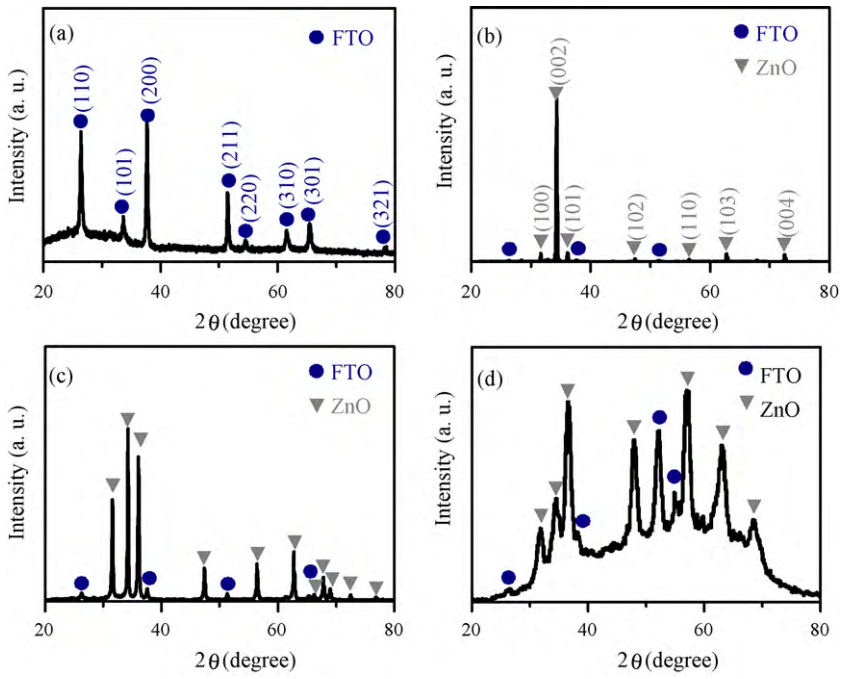

Fig. 4. XRD spectra of (a) a bare FTO glass, (b) highly ordered ZnO nanowires grown on a FTO glass, (c) ZnO nanowire and nanosphere compound structures on a FTO glass, and (d) ZnO nanospheres prepared on a bare FTO glass substrate.

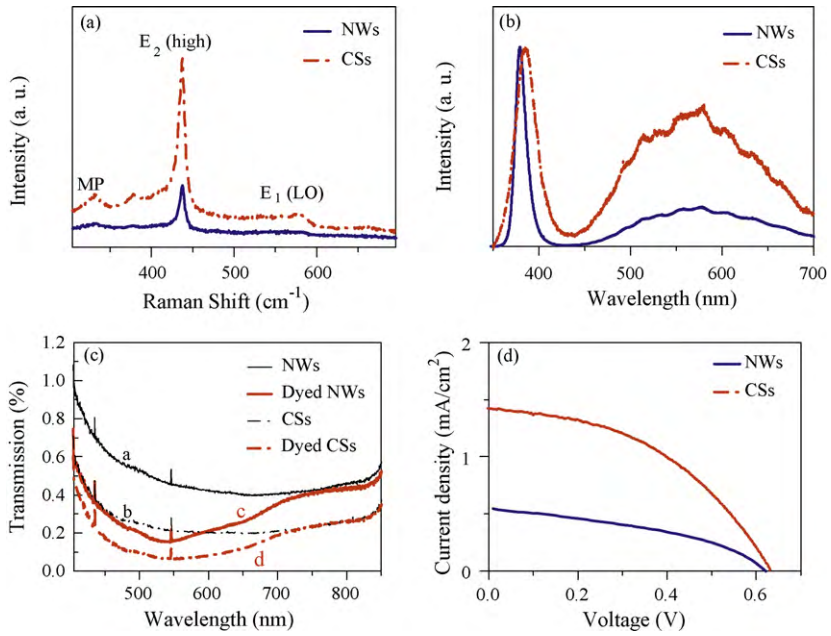

Fig. 5. (a) Raman, (b) PL, and (c) transmission spectra of ZnO nanowires (NWs) and compound structures (CSs). (d) Photocurrent–photovoltage characteristics of the ZnO NW and CS DSSCs.

scattering measurements. The results are shown in Fig. 5(a). From this figure, it is clear that there are high peaks located at 437 cm^{-1}, which are typical Raman active branches corresponding to the nonpolar optical phonon E_2(high) mode of wurtzite ZnO. The other two relatively weak peaks at 332 and 581 cm^{-1} correspond well to the ZnO multiple-phonon (MP) scattering process and E_1 [longitudinal-optical (LO)] mode, respectively [27]. The appearance of the characteristic Raman peaks demonstrates that the obtained ZnO nanostructures are of good crystalline wurtzite structure, which is consistent with the XRD observation.

We have further carried out the room-temperature PL investigation to show the optical properties of the obtained nanostructures. From Fig. 5(b), we note that there are mainly two peaks in the studied samples with a strong ultraviolet (UV) emission at ~380 nm and a relatively weak green peak at ~560 nm. The UV peak could be generally attributed to the near-band-edge emission of the wide-bandgap ZnO, which originates from the recombination of free excitons. Although the origins of the broad visible luminescence are still controversial, it is generally believed that the green emission comes from the recombination of a photogenerated hole with the singly ionized oxygen vacancy [28]. In comparison with the compound nanostructures, the intensities of the green emissions are rather weak in ZnO nanowires, implying the relatively low defects there.

The main reason for the low current density of ZnO nanowire-based DSSCs is that the surface area of the nanorod array is limited. The low surface area of the photoelectrode results in low dye loading and light harvesting. The key point of the present work is that by depositing nanospheres in the interstices between the nanowires to improve the surface area of the photoelectrode and to eventually improve the performance of the ZnO nanostructure-based solar cells. In order to confirm whether or not the introduction of ZnO nanospheres in the photoelectrode enhances the light harvesting, we have also performed the transmission spectroscopy before and after the nanosphere deposition. Fig. 5(c) illustrates the transmission spectra of ZnO nanowires (NWs, curve a) and ZnO compound structures (CSs, curve b), where the transmission of the ZnO compound structures is lower than that of ZnO nanowires. The lower light transmission of the compound structures should be due to the fact that the photoelectrode becomes more compact after depositing nanospheres in the interstices between the nanowires. On the other hand, due to the spherical structure and large size, the nanospheres in the photoelectrode can also act as light scattering center when light passes through the photoelectrode [29].

After dye loading, the dye molecules are adsorbed onto the surface of the ZnO nanostructures. The transmission of the dyed ZnO nanostructures is, as expected, much lower (curves c and d). From Fig. 5(c), it is clear that the transmission corresponding to the dyed compound structures (curve d) is lower than that of the dyed nanowires (curve c). The additional broad absorption peaks at around 535 nm correspond to the absorption of the N719 dye used in the present work [30]. This observation demonstrates unambiguously that, by depositing ZnO nanospheres in the interstices between the nanowires, the fraction of light harvesting is increased, and the performance of the ZnO compound nanostructure-based solar cells is expected to be better than that of ZnO nanowires.

3.4. Application of the obtained ZnO nanostructures in DSSCs

The obtained ZnO nanowires and nanowire/nanosphere compound structures were employed to fabricate the ZnO nanostructure-based DSSCs. We show in Fig. 5(d) the photocurrent density (J)–voltage (V) characteristics of the ZnO nanowire- and compound nanostructure-based DSSCs. It is clear that there is a significant enhancement of the short-circuit current density (from 0.55 to 1.43 mA/cm^2) in the ZnO compound nanostructure-based solar cell, as compared with the ZnO nanowire counterpart. The increase in the short-circuit current density is mainly due to the fact that the surface area of the photoelectrode is increased by depositing nanospheres in the interstices between nanowires (Fig. 3). The increased surface area of the photoelectrode would adsorb much more dye molecules than the ZnO nanowire-based photoelectrode. The light harvesting in the compound nanostructure would increase [Fig. 5(c)], and consequently, more photons would be absorbed in the compound nanostructures, resulting in an increase in the generation of electron-hole pairs and therefore the short-circuit current density. However, the open-circuit voltage does not change much after depositing nanospheres, since it depends on the potential difference between the ZnO photoelectrode and the Pt counter electrode. Although the yielded efficiency

of the ZnO compound nanostructure DSSCs is enhanced to be 0.40% from 0.14% of the ZnO nanowire ones, further work should be on the optimization of the photoelectrode synthesis and DSSC fabrication. For example, in the present DSSC device, a spacer with 100 μm thickness was used but the length of the nanowire is 7.5 μm only. The electrolyte is introduced by capillary action so the contact between the counter electrode and electrolyte may be poor. By decreasing the thickness of the spacer between the two electrodes and using longer nanowires as photoelectrode, we expect significant increase of the overall efficiency of the ZnO compound nanostructure-based solar cell.

4. Conclusions

In summary, we have developed a facile two-step method to prepare ZnO nanowire and nanosphere compound nanostructures. During the synthesis process, we firstly prepare highly ordered nanowires via a chemical route and then use subsequently the first step prepared sample as the substrate for forming ZnO nanowire/nanosphere compound structures. The prepared nanostructures have been successfully used in dye-sensitized solar cells. Compared with the nanowire-based counterpart, the compound nanostructure DSSC exhibits a significant enhancement of the short-circuit current density. We attribute the improved performance to the increased surface area and light scattering of compound nanostructures. Optimized process to prepare the ZnO DSSCs is expected to further enhance the overall efficiency. Although the current work focuses on the synthesis and application of ZnO compound nanostructure in dye-sensitized solar cells, this kind of nanostructures are also expected to be used in other nanodevices such as gas sensor, photocatalyze, and so on, in which high surface area is preferred. The present two-step chemical method opens up possibilities to synthesis of various nanostructures with high surface area for extensive study of the physical and chemical properties of the obtained nanostructures, broadening their potential nanodevice applications.

Acknowledgements

This work was supported by the National Major Basic Research Project of 2010CB933702, Natural Science Foundation of China (Contract No. 10734020), and Shanghai Municipal Commission of Science and Technology Project of 08XD14022.

References

[1] B. O'Regan, M. Grätzel, Nature 353 (1991) 737.
[2] R. Jose, V. Thavasi, S. Ramakrishna, J. Am. Ceram. Soc. 92 (2009) 289.
[3] M. Grätzel, Inorg. Chem. 44 (2005) 6841.
[4] G.K. Mor, O.K. Varghese, M. Paulose, K. Shankar, C.A. Grimes, Sol. Energy Mater. Sol. Cells 90 (2006) 2011.
[5] K. Zhu, N.R. Neale, A. Miedaner, A.J. Frank, Nano Lett. 7 (2007) 69.
[6] M.D. Wei, Y. Konishi, H. Zhou, M. Yanagida, H. Sugihara, H. Arakawa, J. Mater. Chem. 16 (2006) 1287.
[7] M. Duerr, A. Schmid, M. Obermaier, S. Rosselli, A. Yasuda, G. Nelles, Nat. Mater. 4 (2005) 607.
[8] G.K. Mor, K. Shankar, M. Paulose, O.K. Varghese, C.A. Grimes, Nano Lett. 6 (2006) 215.
[9] M. Adachi, Y. Murata, I. Okada, S. Yoshikawa, J. Electrochem. Soc. 150 (2003) G488.
[10] M.Y. Song, Y.R. Ahn, S.M. Jo, D.Y. Kim, J.P. Ahn, Appl. Phys. Lett. 87 (2005) 113113.
[11] H. Rensmo, K. Keis, H. Lindstrom, S. Sodergren, A. Solbrand, A. Hagfeldt, S.E. Lindquist, L.N. Wang, M. Muhammed, J. Phys. Chem. B 101 (1997) 2598.
[12] K. Keis, L. Vayssieres, S.E. Lindquist, A. Hagfeldt, Nanostruct. Mater. 12 (1999) 487.
[13] K. Kakiuchi, E. Hosono, S. Fujihara, J. Photochem. Photobiol. A 179 (2006) 81.
[14] K. Keis, J. Lindgren, S.E. Lindquist, A. Hagfeldt, Langmuir 16 (2000) 4688.
[15] M. Law, L.E. Greene, J.C. Johnson, R. Saykally, P. Yang, Nat. Mater. 4 (2005) 455.
[16] J.B. Baxter, E.S. Aydil, Appl. Phys. Lett. 86 (2005) 053114.
[17] J.B. Baxter, A.M. Walker, K. van Ommering, E.S. Aydil, Nanotechnology 17 (2006) S304.
[18] C.Y. Jiang, X.W. Sun, K.W. Tan, G.Q. Lo, A.K.K. Kyaw, D.L. Kwong, Appl. Phys. Lett. 92 (2005) 143101.
[19] A.D. Pasquier, H.H. Chen, Y.H. Lu, Appl. Phys. Lett. 89 (2006) 253513.
[20] Y.F. Hsu, Y.Y. Xi, A.B. Djurišić, W.K. Chan, Appl. Phys. Lett. 92 (2008) 133507.
[21] C.H. Ku, J.J. Wu, Nanotechnology 18 (2007) 505706.
[22] C.H. Ku, H.H. Yang, G.R. Chen, J.J. Wu, Cryst. Growth. Des. 8 (2008) 283.
[23] Z.R. Tian, J.A. Voigt, J. Liu, B. Mckenzie, M.J. Mcdermott, R.T. Cygan, L.J. Criscenti, Nat. Mater. 2 (2003) 821.
[24] Y.F. Zhu, D.H. Fan, W.Z. Shen, J. Phys. Chem. C 111 (2007) 18629.
[25] V. Thavasi, V. Renugopalakrishnan, R. Jose, S. Ramakrishna, Mater. Sci. Eng., R: Rep. 63 (2009) 81.
[26] P. Li, Y. Wei, H. Liu, X.K. Wang, Chem. Commun. 24 (2004) 2856.
[27] N. Ashkenov, B.N. Mbenkum, C. Bundesmann, V. Riede, M. Lorenz, D. Spemann, E.M. Kaidashev, A. Kasic, M. Schubert, M. Grundmann, G. Wagner, H. Neumann, V. Darakchieva, H. Arwin, B. Monemar, J. Appl. Phys. 93 (2003) 126.
[28] K. Vanheusden, W.L. Warren, C.H. Seager, D.K. Tallant, J.A. Voigt, B.E. Gnade, J. Appl. Phys. 79 (1996) 7983.
[29] J. Ferber, J. Luther, Sol. Energy Mater. Sol. Cells 54 (1998) 265.
[30] A.J. Cheng, Y. Tzeng, Y. Zhou, M. Park, T.H. Wu, C. Shannon, D. Wang, W. Lee, Appl. Phys. Lett. 92 (2008) 092113.